

# Holographic Rényi entropies from hyperbolic black holes with scalar hair

---

Xiaoxuan Bai and Jie Ren

*School of Physics, Sun Yat-sen University, Guangzhou, 510275, China*

*E-mail:* [baixx3@mail2.sysu.edu.cn](mailto:baixx3@mail2.sysu.edu.cn), [renjie7@mail.sysu.edu.cn](mailto:renjie7@mail.sysu.edu.cn)

ABSTRACT: The Rényi entropies as a generalization of the entanglement entropy imply much more information. We analytically calculate the Rényi entropies (with a spherical entangling surface) by means of a class of neutral hyperbolic black holes with scalar hair as a one-parameter generalization of the MTZ black hole. The zeroth-order and third-order phase transitions of black holes lead to discontinuity of the Rényi entropies and their second derivatives, respectively. From the Rényi entropies that are analytic at  $n = \infty$ , we can express the entanglement spectrum as an infinite sum in terms of the Bell polynomials. We show that the analytic treatment is in agreement with numerical calculations for the low-lying entanglement spectrum in a wide range of parameters.

KEYWORDS: AdS-CFT Correspondence, Black Holes in String Theory, Entanglement Spectrum, Holography and Condensed Matter Physics (AdS/CMT)

ARXIV EPRINT: [2210.03732](https://arxiv.org/abs/2210.03732)

---

## Contents

<b>1</b>	<b>Introduction</b>	<b>1</b>
1.1	Rényi entropies from hyperbolic black holes	3
<b>2</b>	<b>Holographic Rényi entropies from hyperbolic AdS<sub>4</sub> black holes</b>	<b>3</b>
2.1	Neutral hyperbolic black holes with scalar hair in AdS <sub>4</sub> spacetime	3
2.2	Holographic Rényi entropies	6
2.3	Some Rényi entropy inequalities	10
<b>3</b>	<b>Holographic Rényi entropies from hyperbolic AdS<sub>5</sub> black holes</b>	<b>10</b>
3.1	Neutral hyperbolic black holes with scalar hair in AdS <sub>5</sub> spacetime	11
3.2	Holographic Rényi entropies	12
<b>4</b>	<b>Entanglement spectrum</b>	<b>14</b>
4.1	Entanglement spectrum from AdS <sub>4</sub> black holes	15
<b>5</b>	<b>Summary and discussion</b>	<b>20</b>
<b>A</b>	<b>Black hole thermodynamics with generalized boundary condition</b>	<b>21</b>
<b>B</b>	<b>Mathematical notes</b>	<b>25</b>
B.1	Inverse Laplace transform	25
B.2	The Bell polynomials	26

---

## 1 Introduction

Entanglement entropy, which measures the entanglement of different parts in a quantum system, has considerable applications in condensed matter physics, e.g., the detection of topological ordered phases [1, 2], quantum phase transitions [3] and fractional quantum Hall effects [4] (see [5, 6] for reviews). Moreover, the holographic description of the entanglement entropy [7, 8] in terms of the AdS/CFT correspondence may inspire a deeper understanding of the quantum gravity [9]. As a generalization of the entanglement entropy, the Rényi entropies [10] imply much more information, e.g., with the Rényi entropies of all orders, the entanglement spectrum [4] (eigenvalue distribution of the reduced density matrix) can be determined [11–15].

A quantum system can be described by a density operator  $\rho$ . For simplicity, we consider a pure state consisting of two subsystems  $A$  and  $B$ , characterized by vectors in Hilbert spaces  $H_A$  and  $H_B$ , respectively. It is convenient to define the reduced density operator  $\rho_A = \text{Tr}_B \rho_{AB}$ , which only depends on the degrees of freedom of  $A$ . The entanglement (von Neumann) entropy is  $S_{EE} = -\text{Tr} \rho_A \log \rho_A$ , which becomes zero when  $\rho_A$  describes a pure

state, or equivalently, the whole system is characterized by  $\rho_{AB} = \rho_A \otimes \rho_B$ . With  $n$  as a parameter, the Rényi entropies are defined as

$$S_n = \frac{1}{1-n} \log \text{Tr}[\rho_A^n], \quad (1.1)$$

which return to the entanglement entropy in the  $n \rightarrow 1$  limit.

Generally, these entropies can be calculated with the replica trick [15–17] in quantum field theory by considering the Euclidean functional integral on  $n$  copies of Riemann surfaces that are matched together. In terms of the AdS/CFT correspondence, the entanglement entropy can be obtained from general relativity by the Ryu-Takayanagi (RT) formula [7, 8]. In particular, for two regions separated by a spherical entangling surface, the Rényi entropies of the ground state can be calculated by means of a hyperbolic (topological) black hole [12, 18] (we briefly review this approach in section 1.1). The temperature of the black hole is related to the Rényi parameter  $n$ , where a larger  $n$  corresponds to a lower temperature.

The hyperbolic Schwarzschild-AdS (SAdS) solution is

$$ds^2 = -\left(-1 - \frac{2M}{r^{d-2}} + \frac{r^2}{L^2}\right) dt^2 + \left(-1 - \frac{2M}{r^{d-2}} + \frac{r^2}{L^2}\right)^{-1} dr^2 + r^2 d\Sigma_{d-1}^2, \quad (1.2)$$

where  $d\Sigma_{d-1}^2 = du^2 + \sinh^2 u d\Omega_{d-2}^2$  is a  $(d-1)$ -dimensional hyperbolic space of unit radius. The hyperbolic SAdS black hole is stable at any temperature [19, 20]. However, if a scalar field is introduced to the system, the black hole may experience a phase transition to the one with scalar hair at a critical temperature. This can be implied from the fact that the IR geometry of the extremal hyperbolic black hole (1.2) includes an  $\text{AdS}_2$  factor, which leads to the Breitenlohner-Freedman bound violated [21]. Accordingly, the Rényi entropies also have a phase transition at a special  $n$ , which has been discussed in [13, 22] in terms of numerical solutions of hairy hyperbolic black holes. In this paper, we provide more analytic calculations.

The Einstein-Maxwell-dilaton (EMD) systems, with gauge field and dilaton field coupled to gravity, have wide applications in gauge/gravity duality. An especially useful class of analytic solutions of the EMD systems was found in [23], with special cases belonging to gauged supergravity. In a particular neutral limit, the gauge field vanishes while the dilaton field is kept, resulting in neutral hyperbolic black holes with scalar hair [24]. These black holes have zeroth-order and third-order phase transitions, and the corresponding Rényi entropies and their second derivatives show discontinuity, respectively.

With the analytic solutions of the Einstein-scalar systems in hand, we explicitly obtain the Rényi entropies  $S_n$  and calculate the entanglement spectrum. For the one-parameter family of our systems, these Rényi entropies converge to the same entanglement entropy in the  $n \rightarrow 1$  limit. For special cases, we find that the Rényi entropies have the same  $(1+1/n)$  factor as the universal result in 2D CFTs. Starting with the analytic Rényi entropies, we can calculate the entanglement spectrum by an inverse Laplace transform. Consequently, we can express the entanglement spectrum in terms of an infinite sum. By truncating this sum, we can verify that it is consistent with the numerical calculation for a wide range of eigenvalues.

The paper is organized as follows. In section 2, we begin by introducing a class of neutral hyperbolic black holes with scalar hair [24] in AdS<sub>4</sub> spacetime and refining their thermodynamics and stability analysis. Then we calculate holographic Rényi entropies and discuss corresponding phase transitions. Besides, we verify some Rényi entropy inequalities in terms of the thermodynamically preferred solution. In section 3, we generalize these calculations to higher dimensions. In section 4, we calculate the entanglement spectrum from the Rényi entropies as an infinite sum in terms of the Bell polynomials and discuss its validity by comparing it with additional numerical calculations. In appendix A, we give the boundary counter terms for holographic renormalization, from which we obtain the mass and free energy of the hyperbolic black holes. In appendix B, we give a brief note on the mathematics related to our calculations, including the inverse Laplace transform and the exponential Bell polynomials.

### 1.1 Rényi entropies from hyperbolic black holes

For the case with a spherical entangling surface, we can calculate the Rényi entropies by conformally mapping the causal development of the enclosed region to a hyperbolic cylinder  $\mathbb{R} \times \mathbb{H}^{d-1}$  (see [12, 18] for details). Assuming that the radius of the entangling sphere is  $L$ , then the corresponding hyperbolic space  $\mathbb{H}^{d-1}$  also has the radius  $L$ . Under this conformal transformation, the reduced density matrix is acted by a unitary operator

$$\rho = U \frac{e^{-H/T_0}}{Z(T_0)} U^{-1}, \quad (1.3)$$

where  $H$  is the modular Hamiltonian generating the (Rindler) time translation on  $\mathbb{R} \times \mathbb{H}^{d-1}$ , and  $Z(T_0) = \text{Tr}[e^{H/T_0}]$  is the thermal partition function at temperature  $T_0 = 1/2\pi L$ . Thus,

$$\text{Tr}[\rho^n] = \frac{Z(T_0/n)}{Z(T_0)^n}, \quad (1.4)$$

from which the Rényi entropies can be calculated from the thermodynamics of the CFT living on the hyperbolic cylinder  $\mathbb{R} \times \mathbb{H}^{d-1}$ . In terms of the AdS/CFT correspondence, the partition function  $Z(T_0/n)$  is identified with that of a hyperbolic black hole at temperature  $T = T_0/n$ . Thus, the Rényi entropies can be calculated by means of the hyperbolic black hole. Furthermore, with the free energy  $F = -T \log Z$  of black holes, we can rewrite the Rényi entropies as

$$S_n = \frac{n}{1-n} \frac{1}{T_0} [F(T_0) - F(T_0/n)]. \quad (1.5)$$

Equivalently, with the relation  $S_{\text{therm}} = -\partial F / \partial T$ , we can obtain

$$S_n = \frac{n}{n-1} \frac{1}{T_0} \int_{T_0/n}^{T_0} S_{\text{therm}}(T) dT. \quad (1.6)$$

## 2 Holographic Rényi entropies from hyperbolic AdS<sub>4</sub> black holes

### 2.1 Neutral hyperbolic black holes with scalar hair in AdS<sub>4</sub> spacetime

To study holographic Rényi entropies, we employ a class of neutral hyperbolic black holes with scalar hair [24] as a one-parameter family generalization of the MTZ black hole [25].

The action is

$$S = \int d^4x \sqrt{-g} \left[ R - \frac{1}{2}(\partial\phi)^2 - V(\phi) \right], \quad (2.1)$$

with the potential (first found in [23])

$$V(\phi) = -\frac{2}{(1+\alpha^2)^2 L^2} \left[ \alpha^2 (3\alpha^2 - 1) e^{-\phi/\alpha} + 8\alpha^2 e^{(\alpha-1/\alpha)\phi/2} + (3-\alpha^2) e^{\alpha\phi} \right], \quad (2.2)$$

where  $\alpha$  is a parameter, and the potential equals the cosmological constant when  $\alpha = 0$  or  $\alpha \rightarrow \infty$ . A remarkable feature of this potential is that it interpolates among four scalar potentials in supergravity: the values  $\alpha = 0, 1/\sqrt{3}, 1,$  and  $\sqrt{3}$  correspond to special cases of STU supergravity. Since the  $\phi \rightarrow 0$  behavior is  $V(\phi) = -6/L^2 - (1/L^2)\phi^2 + \mathcal{O}(\phi^4)$ , the mass of the scalar field satisfies  $m^2 L^2 = -2$ . From the relation  $m^2 L^2 = \Delta(\Delta - d)$ , where  $d = 3$ , the scaling dimension of the dual operator in the CFT is  $\Delta_+ = 2$  or  $\Delta_- = 1$ .<sup>1</sup>

The solution to the system is [24]

$$ds^2 = -f(r)dt^2 + \frac{dr^2}{f(r)} + U(r)d\Sigma_2^2, \quad e^{\alpha\phi} = \left(1 - \frac{b}{r}\right)^{\frac{2\alpha^2}{1+\alpha^2}}, \quad (2.3)$$

with

$$f(r) = -\left(1 - \frac{b}{r}\right)^{\frac{1-\alpha^2}{1+\alpha^2}} + \frac{r^2}{L^2} \left(1 - \frac{b}{r}\right)^{\frac{2\alpha^2}{1+\alpha^2}}, \quad U(r) = r^2 \left(1 - \frac{b}{r}\right)^{\frac{2\alpha^2}{1+\alpha^2}}. \quad (2.4)$$

This solution was obtained by taking a nontrivial neutral limit<sup>2</sup> from a class of charged dilaton black hole solutions in [23]. The horizon radius of black holes is obtained by taking  $f(r_h) = 0$ , and the parameter  $b$  can be replaced by  $r_h$  with

$$b = r_h \left[ 1 - \left(\frac{r_h}{L}\right)^{\frac{2(1+\alpha^2)}{1-3\alpha^2}} \right]. \quad (2.5)$$

Now we refine the analysis of the black hole thermodynamics studied in [24]. The temperature is

$$T = \frac{f'(r_h)}{4\pi} = \frac{1}{4\pi(1+\alpha^2)L} \left[ (3-\alpha^2) \left(\frac{r_h}{L}\right)^{\frac{1+\alpha^2}{1-3\alpha^2}} - (1-3\alpha^2) \left(\frac{r_h}{L}\right)^{-\frac{1+\alpha^2}{1-3\alpha^2}} \right], \quad (2.6)$$

from which we can solve  $r_h$  in terms of temperature as

$$r_{h,\pm} = \left( \frac{2\pi L T (1+\alpha^2) \pm \sqrt{4\pi^2 L^2 T^2 (1+\alpha^2)^2 + (3-\alpha^2)(1-3\alpha^2)}}{3-\alpha^2} \right)^{\frac{1-3\alpha^2}{1+\alpha^2}} L, \quad (2.7)$$

<sup>1</sup>The asymptotic behavior of the scalar field near the AdS boundary is determined by its mass. If we use Fefferman-Graham (FG) coordinates, the asymptotic expansion is  $\phi(x, z) = z^{\Delta_-}(\phi_a + \phi_b z + \dots)$  for the alternative quantization. We consider a sourceless boundary condition corresponding to a triple-trace deformation in the dual CFT [27]. Specifically, the boundary condition for the following solution is given by  $\phi_b/\phi_a^2 = \tau$ , where  $\tau = -(1-\alpha^2)/4\alpha$ .

<sup>2</sup>There is also a trivial neutral limit, which gives the SAdS black hole [24].

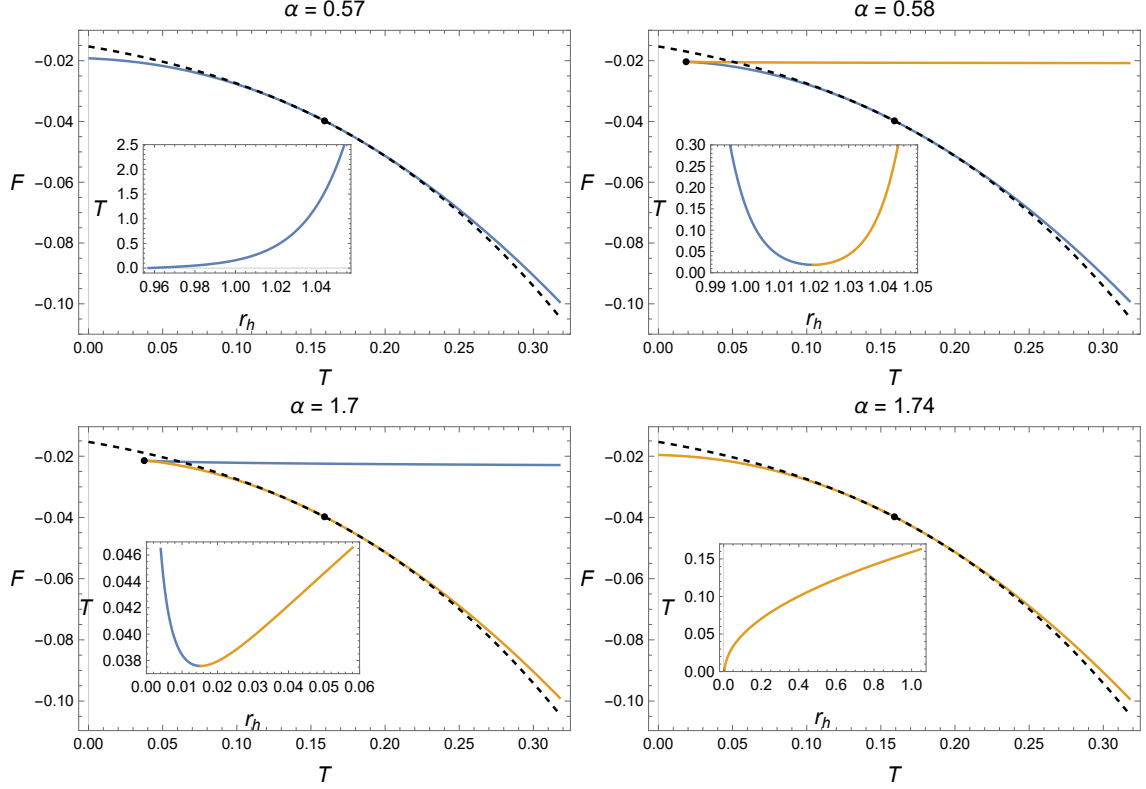


**Figure 1.** The free energy as a function of temperature for different values of  $\alpha$ . The dashed line is for the SAdS black hole, while the solid line is for the hairy black hole, where the blue one is for  $r_{h,+}$  and the orange one is for  $r_{h,-}$ . The subfigure describes the relation between the temperature and horizon radius. In all figures, we have set  $L = G = V_\Sigma = 1$ .

which shows that there may be two solutions of black holes at a given temperature, and the horizon radius is distinguished by  $r_{h,\pm}$ . More specifically, when  $0 \leq \alpha \leq 1/\sqrt{3}$ , only  $r_{h,+}$  is real; when  $\alpha \geq \sqrt{3}$ , only  $r_{h,-}$  is real; when  $1/\sqrt{3} < \alpha < \sqrt{3}$ , both  $r_{h,\pm}$  are real. The two solutions can be seen in figure 1. The temperature can reach zero when  $\alpha \leq 1/\sqrt{3}$  or  $\alpha \geq \sqrt{3}$ . However, when  $1/\sqrt{3} < \alpha < \sqrt{3}$ , there is a minimum temperature above zero,

$$T_m = \frac{\sqrt{(3 - \alpha^2)(3\alpha^2 - 1)}}{2\pi(1 + \alpha^2)L}, \quad (2.8)$$

at which the two solutions intersect. In a special case  $\alpha = 1$ , the  $T_m$  has a maximum value  $T_0 = 1/2\pi L$ .

The Bekenstein-Hawking entropy is given by

$$S = \frac{V_\Sigma}{4G} U(r_h) = \frac{V_\Sigma}{4G} \left( \frac{r_h}{L} \right)^{\frac{2(1-\alpha^2)}{1-3\alpha^2}} L^2, \quad (2.9)$$

where  $V_\Sigma$  is the (regulated) area of the hyperbolic space  $d\Sigma_2^2$ . With a boundary condition corresponding to a triple-trace deformation in the dual CFT [24, 26], the mass derived from

the holographic renormalization is

$$M = -\frac{V_\Sigma}{8\pi G} \frac{1-\alpha^2}{1+\alpha^2} b = -\frac{V_\Sigma}{8\pi G} \frac{1-\alpha^2}{1+\alpha^2} r_h \left[ 1 - \left( \frac{r_h}{L} \right)^{\frac{2(1+\alpha^2)}{1-3\alpha^2}} \right]. \quad (2.10)$$

All thermodynamic quantities above can be expressed as functions of temperature by means of (2.7). So we can easily verify the first law of thermodynamics in the canonical ensemble:  $dM = TdS$ . Finally, the Helmholtz free energy is

$$F = M - TS = -\frac{V_\Sigma}{16\pi G} r_h \left[ 1 + \left( \frac{r_h}{L} \right)^{\frac{2(1+\alpha^2)}{1-3\alpha^2}} \right]. \quad (2.11)$$

A more rigorous treatment of the black hole thermodynamics is in appendix A, in which the boundary counter terms are given together with the boundary condition of the scalar field.

The stability of black holes can be analyzed by comparing the free energy of black holes with and without scalar hair. Note that when  $\alpha = 0$ , the black hole is the SAdS black hole. For representative cases of  $\alpha$ , we plot the free energy as a function of temperature in figure 1. The SAdS black hole is always more stable than the hairy black hole at  $T > T_0$ . As the temperature is decreased, we draw the following conclusions on phase transitions:

- $0 < \alpha < 1$ : The SAdS black hole experiences a third-order phase transition to the hairy one with the horizon size  $r_{h,+}$  at  $T = T_0$ .
  - $0 < \alpha \leq 1/\sqrt{3}$ : There is only one hairy black hole corresponding to  $r_{h,+}$ .
  - $1/\sqrt{3} < \alpha < 1$ : The stable hairy black hole corresponds to  $r_{h,+}$ , while an unstable branch corresponds to  $r_{h,-}$ . A zeroth-order phase transition to the SAdS black hole occurs at  $T_m$ .
- $\alpha = 1$ : The SAdS black hole is always more stable than the hairy black hole.
- $\alpha > 1$ : The SAdS black hole experiences a third-order phase transition to the hairy one with the horizon size  $r_{h,-}$  at  $T = T_0$ .
  - $1 < \alpha < \sqrt{3}$ : The stable hairy black hole corresponds to  $r_{h,-}$ , while an unstable branch corresponds to  $r_{h,+}$ . A zeroth-order phase transition to the SAdS black hole occurs at  $T_m$ .
  - $\alpha \geq \sqrt{3}$ : There is only one hairy black hole corresponding to  $r_{h,-}$ .

## 2.2 Holographic Rényi entropies

We calculate the Rényi entropies from the free energy by (1.5) (the thermal entropy calculation (1.6) gives the same result). The expression (1.5) also describes the Rényi entropies with phase transitions but should be treated carefully. We need to take the thermodynamically preferred solution to calculate the free energy and entropy at temperature  $T_0$  and  $T_0/n$ . Notably, the Rényi entropies with  $n < 1$  for any  $\alpha$  are the same as those from the

SAdS black hole, since the most stable solution is always the SAdS black hole when  $T > T_0$  (see figure 1).

We first obtain the Rényi entropies calculated from the hairy black holes without taking into account phase transitions to the SAdS black hole,

$$S_n = \frac{nL^2}{8(n-1)G} \left[ 2 - \mathcal{S}_\pm(\alpha, n)^{\frac{1-3\alpha^2}{1+\alpha^2}} - \mathcal{S}_\pm(\alpha, n)^{\frac{3-\alpha^2}{1+\alpha^2}} \right] V_\Sigma, \quad (2.12)$$

where

$$\mathcal{S}_\pm(\alpha, n) = \frac{1}{(3-\alpha^2)n} \left[ (1+\alpha^2) \pm \sqrt{(1+\alpha^2)^2 + (3-\alpha^2)(1-3\alpha^2)n^2} \right]. \quad (2.13)$$

Here  $\mathcal{S}_\pm$  correspond to the two solutions  $r_{h,\pm}$ :  $\mathcal{S}_+$  is for  $0 \leq \alpha \leq 1$  and  $\mathcal{S}_-$  is for  $\alpha \geq 1$ . Clearly,  $S_n$  is an analytic function of  $n$  with a parameter  $\alpha$ . The Rényi entropies from the SAdS black hole are given by  $S_n(\alpha = 0)$ .

We use  $\bar{S}_n$  to denote the Rényi entropies with phase transitions, and it is non-analytic at  $n$  corresponding to the phase transition temperature of the black holes,  $T = T_0/n = (2\pi Ln)^{-1}$ . When  $0 < \alpha \leq 1/\sqrt{3}$  and  $\alpha \geq \sqrt{3}$ , the Rényi entropies are given by

$$\bar{S}_n = \begin{cases} S_n(\alpha = 0), & n \leq 1, \\ S_n, & n > 1, \end{cases} \quad (2.14)$$

where  $S_n$  are the Rényi entropies from hairy black holes given by (2.12). The phase transition occurs at  $n = 1$  ( $T = T_0$ ), at which  $\bar{S}_n$  is continuous, while its second derivative  $\partial_n^2 \bar{S}_n$  is discontinuous. When  $1/\sqrt{3} < \alpha < \sqrt{3}$ , the Rényi entropies are given by

$$\bar{S}_n = \begin{cases} S_n(\alpha = 0), & n \leq 1 \text{ or } n \geq n_m, \\ S_n, & 1 < n < n_m, \end{cases} \quad (2.15)$$

where  $n_m$  is the critical parameter of the Rényi entropies derived from (2.8),

$$n_m = \frac{T_0}{T_m} = \frac{1+\alpha^2}{\sqrt{(3-\alpha^2)(3\alpha^2-1)}} \geq 1. \quad (2.16)$$

Besides the phase transition at  $n = 1$ , the Rényi entropies  $\bar{S}_n$  are discontinuous at  $n = n_m$ .

From (2.13), we have  $\lim_{n \rightarrow 1} \mathcal{S}_\pm(\alpha, n) = 1$ , so the  $n \rightarrow 1$  limit of the Rényi entropies (for any  $\alpha$ ) gives

$$S_{EE} = \frac{L^2}{4G} V_\Sigma, \quad (2.17)$$

which means that the scalar field does not affect the entanglement entropy ( $n = 1$ ), while it affects the Rényi entropies with  $n > 1$ . Moreover, the Rényi entropies also satisfy an area law [28]

$$n^2 \partial_n \left( \frac{n-1}{n} S_n \right) = \frac{\text{Area}(\text{Brane}_n)}{4G} = \frac{L^2}{4G} \mathcal{S}_\pm(\alpha, n)^{\frac{2(1-\alpha^2)}{1+\alpha^2}} V_\Sigma, \quad (2.18)$$

where the  $\text{Brane}_n$  is a bulk codimension-2 cosmic brane homologous to the entangling region A,<sup>3</sup> and the brane tension is  $T_n = (n-1)/4nG$ . Since  $\lim_{n \rightarrow 1} \mathcal{S}_\pm(\alpha, n) = 1$  and

<sup>3</sup>Here A is the region enclosed by the spherical entangling surface.



$\lim_{n \rightarrow 1} T_n = 0$ , the one-parameter generalized area law will reduce to the RT formula in the  $n \rightarrow 1$  limit. It is straightforward to verify that (2.18) is exactly the entropy of the hyperbolic black hole.

The Rényi entropies as a function of  $n$  for different values  $\alpha$  are plotted in figure 2. The most notable cases are when  $\alpha$  takes values corresponding to special cases of STU supergravity.<sup>4</sup> We use the same terminology as in [24]:

- 1-charge black hole ( $\alpha = \sqrt{3}$ )

This black hole is exactly the MTZ black hole. The free energy is

$$F = -\frac{L}{16\pi G}(1 + 4\pi^2 L^2 T^2)V_\Sigma. \quad (2.19)$$

From (1.5), the Rényi entropies are

$$S_n = \frac{L^2}{8G}\left(1 + \frac{1}{n}\right)V_\Sigma, \quad (2.20)$$

for  $n \geq 1$ . Note that the result has the same  $n$  dependence as the universal result in 2D CFTs with a single interval [16],

$$S_n(D=2) = \frac{c}{6}\left(1 + \frac{1}{n}\right)\log \frac{l}{\delta}, \quad (2.21)$$

where  $c$  is the central charge,  $\delta$  is a short-distance cut-off, and  $l$  is the size of the interval. Besides, (2.20) or (2.21) can also be derived from the SAdS<sub>3</sub> hyperbolic black hole [12].

- 2-charge black hole ( $\alpha = 1$ )

In this case, the free energy is linear with the temperature

$$F = -\frac{L^2}{4G}TV_\Sigma, \quad (2.22)$$

which is always less stable than the SAdS black hole. So the Rényi entropies are  $S_n = S_n(\alpha = 0)$ .

- 3-charge black hole ( $\alpha = 1/\sqrt{3}$ )

The system (2.1)–(2.4) has an invariance under  $\alpha \rightarrow 1/\alpha$  and  $b \rightarrow -b$ . So the free energy and Rényi entropies are the same as (2.19) and (2.20), respectively. As a remark, for an EMD system with the potential (2.2), the  $\alpha = 1/\sqrt{3}$  case is also called the Gubser-Rocha model, and the extremal near-horizon geometry of its 11-dimensional lift has an AdS<sub>3</sub> factor [30].

---

<sup>4</sup>There are U(1)<sup>4</sup> gauged fields in STU supergravity for AdS<sub>4</sub> spacetime [29], with four U(1) charges, respectively. Here the special values of  $\alpha$  correspond to the cases when some of the charges are the same while others are zero (see [24] for more details).

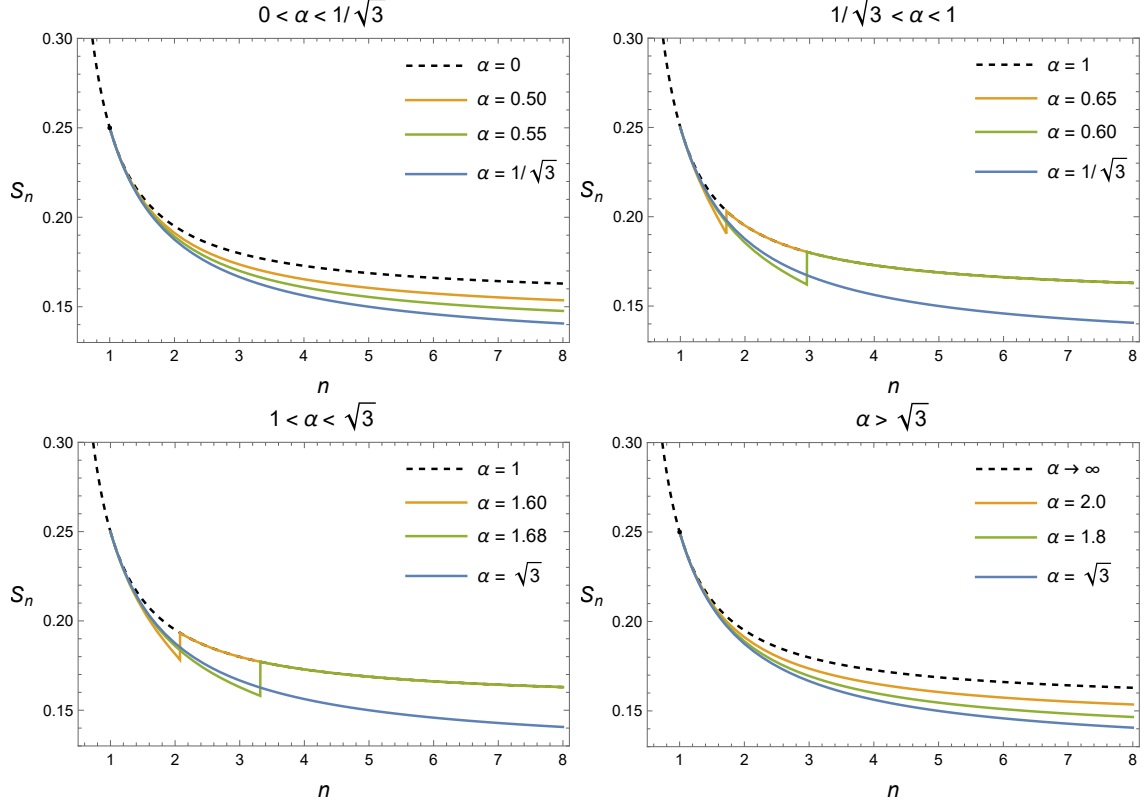


**Figure 2.** The Rényi entropies as a function of  $n$  for different values of  $\alpha$  (AdS<sub>4</sub>). The dashed line is for the SAdS<sub>4</sub> case, and the blue line is for  $\alpha = 1/\sqrt{3}$  or  $\sqrt{3}$ . A third-order phase transition occurs at  $n = 1$  (for all  $\alpha \neq 1$ ), where the second derivative has discontinuity. When  $1/\sqrt{3} < \alpha < \sqrt{3}$ , a zeroth-order phase transition of black holes leads to discontinuity of the Rényi entropies at  $n_m > 1$ .

- 4-charge black hole ( $\alpha = 0$ )

The black hole is the SAdS black hole. The free energy is

$$F = -\frac{L}{108\pi G} [\pi L T (9 + 8\pi^2 L^2 T^2) + (3 + 4\pi^2 L^2 T^2)^{3/2}] V_\Sigma. \quad (2.23)$$

The Rényi entropies are

$$S_n(\alpha = 0) = \frac{nL^2}{8(n-1)G} \left[ 2 - \frac{1 + \sqrt{1 + 3n^2}}{3n} - \left( \frac{1 + \sqrt{1 + 3n^2}}{3n} \right)^3 \right] V_\Sigma, \quad (2.24)$$

which exactly gives the result from the SAdS<sub>4</sub> black hole in [12].

### 2.3 Some Rényi entropy inequalities

The Rényi entropies should satisfy the following inequalities [31]

$$\frac{\partial S_n}{\partial n} \leq 0, \quad (2.25)$$

$$\frac{\partial}{\partial n} \left( \frac{n-1}{n} S_n \right) \geq 0, \quad (2.26)$$

$$\frac{\partial}{\partial n} ((n-1)S_n) \geq 0, \quad (2.27)$$

$$\frac{\partial^2}{\partial n^2} ((n-1)S_n) \leq 0. \quad (2.28)$$

From the holographic calculation, these inequalities are closely related to the stability of hyperbolic black holes (or the CFT living on the hyperbolic cylinder), which has been discussed<sup>5</sup> in detail in [12] by combining these inequalities with (1.6). Among them, (2.25) and (2.28) are ensured by the positive specific heat of black holes, while (2.26) is guaranteed by the positivity of thermal entropy. Besides, (2.27) is related to both specific heat and thermal entropy.

We can verify that all these inequalities are satisfied for the Rényi entropies that we obtained from the thermodynamically preferred branch of black hole solutions. The thermal entropy is positive from (2.9) since  $r_h > 0$ . The specific heat can be derived from (2.7) and (2.9) as

$$c = T \frac{\partial S}{\partial T} = \pm \frac{V_\Sigma}{G} \frac{\pi(1-\alpha^2)L^3 T}{\sqrt{4\pi^2 L^2 T^2 (1+\alpha^2)^2 + (3-\alpha^2)(1-3\alpha^2)}} \left( \frac{r_{h,\pm}}{L} \right)^{\frac{2(1-\alpha^2)}{1-3\alpha^2}}. \quad (2.29)$$

As discussed in section 2.1, the thermodynamically preferred solution is either the SAdS black hole or one of the hairy branches, which depends on the values of  $\alpha$  and the Rényi parameter  $n$ . The specific heat of the SAdS solution is obvious to see by taking  $\alpha = 0$  ( $r_{h,+}$ ). Between the two hairy black hole branches, the one with  $r_{h,+}$  is more stable when  $0 < \alpha < 1$ , while the one  $r_{h,-}$  is more stable when  $\alpha > 1$ . Thus the specific heat is always positive for the more stable hairy solution. When  $\alpha = 1$ , the hairy black hole is unstable with zero specific heat, so the black hole is always SAdS. Therefore, these Rényi entropy inequalities hold for all values of  $\alpha$  (except for the critical points where the derivatives of the Rényi entropies are discontinuous).

### 3 Holographic Rényi entropies from hyperbolic AdS<sub>5</sub> black holes

It is natural to generalize the AdS<sub>4</sub> cases to higher dimensions, especially AdS<sub>5</sub>, whose special cases also correspond to supergravity. A class of black hole solutions to the EMD system in higher dimensions were found in [33, 34]. We still focus on the nontrivial neutral limit [24].

---

<sup>5</sup>These inequalities can also be proved under the assumption of bulk stability against perturbation [32] through the holographic description of the Rényi entropies in [28].

### 3.1 Neutral hyperbolic black holes with scalar hair in AdS<sub>5</sub> spacetime

The action in AdS<sub>5</sub> is

$$S = \int d^5x \sqrt{-g} \left[ R - \frac{1}{2} (\partial\phi)^2 - V(\phi) \right], \quad (3.1)$$

with the potential<sup>6</sup>

$$V(\phi) = -\frac{12}{(4+3\alpha^2)^2 L^2} \left[ 3\alpha^2(3\alpha^2-2)e^{-\frac{4\phi}{3\alpha}} + 36\alpha^2 e^{\frac{(3\alpha^2-4)\phi}{6\alpha}} + 2(8-3\alpha^2)e^{\alpha\phi} \right]. \quad (3.2)$$

The solution is [24]

$$ds^2 = -f(r)dt^2 + \frac{dr^2}{g(r)} + U(r)d\Sigma_3^2, \quad e^{\alpha\phi} = \left(1 - \frac{b^2}{r^2}\right)^{\frac{6\alpha^2}{4+3\alpha^2}}, \quad (3.3)$$

with

$$\begin{aligned} f(r) &= -\left(1 - \frac{b^2}{r^2}\right)^{\frac{4-3\alpha^2}{4+3\alpha^2}} + \frac{r^2}{L^2} \left(1 - \frac{b^2}{r^2}\right)^{\frac{3\alpha^2}{4+3\alpha^2}}, \\ g(r) &= f(r) \left(1 - \frac{b^2}{r^2}\right)^{\frac{3\alpha^2}{4+3\alpha^2}}, \quad U(r) = r^2 \left(1 - \frac{b^2}{r^2}\right)^{\frac{3\alpha^2}{4+3\alpha^2}}. \end{aligned} \quad (3.4)$$

From  $f(r_h) = 0$ , the parameter  $b^2$  can be replaced with

$$b^2 = r_h^2 \left[ 1 - \left(\frac{r_h}{L}\right)^{\frac{4+3\alpha^2}{2-3\alpha^2}} \right], \quad (3.5)$$

and thus the temperature is

$$T = \frac{\sqrt{f'(r_h)g'(r_h)}}{4\pi} = \frac{1}{2\pi(4+3\alpha^2)L} \left[ (8-3\alpha^2) \left(\frac{r_h}{L}\right)^{\frac{4+3\alpha^2}{4-6\alpha^2}} - (4-6\alpha^2) \left(\frac{r_h}{L}\right)^{-\frac{4+3\alpha^2}{4-6\alpha^2}} \right]. \quad (3.6)$$

So we have

$$r_{h,\pm} = \left( \frac{\pi L T (4+3\alpha^2) \pm \sqrt{\pi^2 L^2 T^2 (4+3\alpha^2)^2 + (8-3\alpha^2)(4-6\alpha^2)}}{8-3\alpha^2} \right)^{\frac{4-6\alpha^2}{4+3\alpha^2}} L. \quad (3.7)$$

Other thermodynamic quantities are

$$M = -\frac{3V_\Sigma}{16\pi G} \frac{4-3\alpha^2}{4+3\alpha^2} r_h^2 \left[ 1 - \left(\frac{r_h}{L}\right)^{\frac{4+3\alpha^2}{2-3\alpha^2}} \right], \quad (3.8)$$

$$S = \frac{V_\Sigma}{4G} U(r_h)^{3/2} = \frac{V_\Sigma}{4G} \left(\frac{r_h}{L}\right)^{\frac{3(4-3\alpha^2)}{2(2-3\alpha^2)}} L^3, \quad (3.9)$$

$$F = M - TS = -\frac{V_\Sigma}{16\pi G} r_h^2 \left[ 1 + \left(\frac{r_h}{L}\right)^{\frac{4+3\alpha^2}{2-3\alpha^2}} \right], \quad (3.10)$$

<sup>6</sup>The expansion of the potential near  $\phi \rightarrow 0$  is  $V(\phi) = -12/L^2 - 2\phi^2/L^2 + \mathcal{O}(\phi^3)$ , so the mass of the scalar field is  $m^2 L^2 = -4$  and the scaling dimension of the dual operator is  $\Delta_\pm = 2$ . The scalar field behaves as  $\phi(r) \sim \phi_a \ln r/r^2 + \phi_b/r^2$  near the AdS boundary. The boundary condition for the following solution corresponds to the standard quantization  $\phi_a = 0$ .

from which we can verify the phase transitions and the Rényi entropy inequalities as in section 2.

Similar to the discussion in AdS<sub>4</sub> cases, (3.7) shows that there may be two solutions of black holes at a given temperature:  $r_{h,+}$  is real when  $0 \leq \alpha < 4/\sqrt{6}$ , while  $r_{h,-}$  is real when  $\alpha > 2/\sqrt{6}$ . The temperature can reach zero when  $0 \leq \alpha \leq 2/\sqrt{6}$  or  $\alpha \geq 4/\sqrt{6}$ , while there is a minimum temperature when  $2/\sqrt{6} < \alpha < 4/\sqrt{6}$ ,

$$T_m = \frac{\sqrt{2(3\alpha^2 - 2)(8 - 3\alpha^2)}}{\pi(3\alpha^2 + 4)L}, \quad (3.11)$$

at which a zeroth-order phase transition from hairy black holes to the SAdS black hole occurs. The maximum value of  $T_m$  is  $T_0 = 1/2\pi L$  in the case  $\alpha = 2/\sqrt{3}$ . Besides, there is a third-order phase transition from the SAdS hole to hairy black holes at  $T = T_0$  for any  $\alpha \neq 2/\sqrt{3}$ .

### 3.2 Holographic Rényi entropies

The calculation of the Rényi entropies is similar to that in section 2. We first obtain the result from hairy black holes without taking in to account phase transitions,

$$S_n = \frac{nL^3}{8(n-1)G} \left[ 2 - \mathcal{S}_\pm(\alpha, n)^{\frac{8-12\alpha^2}{4+3\alpha^2}} - \mathcal{S}_\pm(\alpha, n)^{\frac{16-6\alpha^2}{4+3\alpha^2}} \right] V_\Sigma, \quad (3.12)$$

where

$$\mathcal{S}_\pm(\alpha, n) = \frac{1}{2(8-3\alpha^2)n} \left[ (4+3\alpha^2) \pm \sqrt{(4+3\alpha^2)^2 + 8(8-3\alpha^2)(2-3\alpha^2)n^2} \right], \quad (3.13)$$

where the  $\pm$  signs correspond to  $r_{h,\pm}$  similar to AdS<sub>4</sub> cases. With phase transitions, the Rényi entropies  $\bar{S}_n$  is non-analytic at  $n$  corresponding to the phase transition temperature of the black holes. When  $0 < \alpha \leq 2/\sqrt{6}$  and  $\alpha \geq 4/\sqrt{6}$ , the Rényi entropies  $\bar{S}_n$  are given by (2.14), in which  $S_n$  is (3.12). When  $2/\sqrt{6} < \alpha < 4/\sqrt{6}$ , the Rényi entropies  $\bar{S}_n$  are given by (2.15) with the critical parameter

$$n_m = \frac{T_0}{T_m} = \frac{4+3\alpha^2}{\sqrt{2(3\alpha^2-2)(8-3\alpha^2)}}. \quad (3.14)$$

The Rényi entropies as a function of  $n$  for different values  $\alpha$  are plotted in figure 3. The black holes corresponding to special cases of supergravity are:<sup>7</sup>

- 1-charge black hole ( $\alpha = 4/\sqrt{6}$ )

We find the free energy when  $\alpha = 4/\sqrt{6}$  in AdS<sub>5</sub> is exactly the same as the one when  $\alpha = \sqrt{3}$  in AdS<sub>4</sub>. The results are

$$F = -\frac{L^2}{16\pi G} (1 + 4\pi^2 L^2 T^2) V_\Sigma, \quad S_n = \frac{L^3}{8G} \left( 1 + \frac{1}{n} \right) V_\Sigma. \quad (3.15)$$

<sup>7</sup>Unlike the AdS<sub>4</sub> cases with the four U(1) gauge fields, there are three U(1) gauge fields in AdS<sub>5</sub> in STU supergravity [29], and thus we have three U(1) charges here.

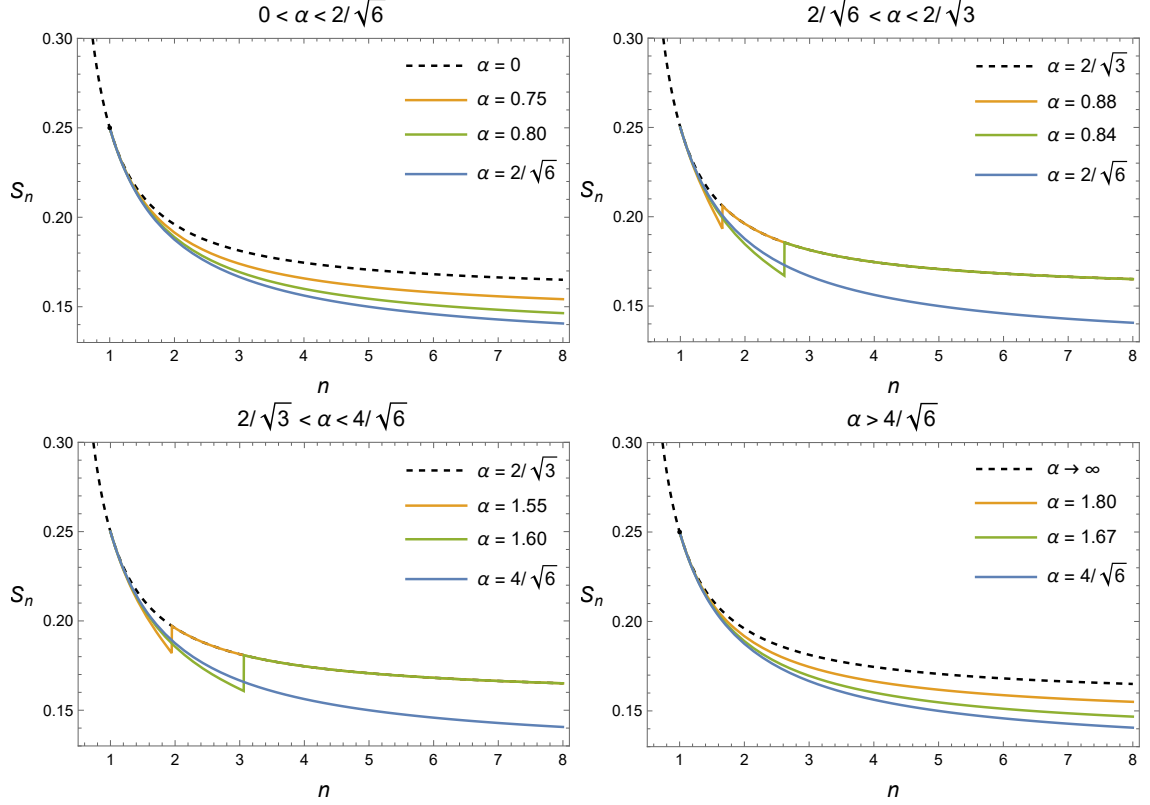


**Figure 3.** The Rényi entropies as a function of  $n$  for different values of  $\alpha$  (AdS<sub>5</sub>). The dashed line is for the SAdS<sub>5</sub> case, and the blue line is for  $\alpha = 2/\sqrt{6}$  or  $4/\sqrt{6}$ . A third-order phase transition occurs at  $n = 1$  (for all  $\alpha \neq 2/\sqrt{3}$ ), where the second derivative has discontinuity. When  $2/\sqrt{6} < \alpha < 4/\sqrt{6}$ , a zeroth-order phase transition of black holes leads to discontinuity of the Rényi entropies at  $n_{\text{m}} > 1$ .

- 2-charge black hole ( $\alpha = 2/\sqrt{6}$ )

This solution corresponds to the same system with the 1-charge black hole (3.15).

- 3-charge black hole ( $\alpha = 0$ )

The scalar hair vanishes, and we obtain the SAdS<sub>5</sub> black hole with the free energy

$$F = -\frac{L^2}{128\pi G} \left[ 6 + 4\pi LT \left( \pi LT(3 + \pi^2 L^2 T^2) + (2 + \pi^2 L^2 T^2)^{3/2} \right) \right] V_{\Sigma}. \quad (3.16)$$

And the Rényi entropies are

$$S_n(\alpha = 0) = \frac{nL^3}{8(n-1)G} \left[ 2 - \left( \frac{1 + \sqrt{1 + 8n^2}}{4n} \right)^2 - \left( \frac{1 + \sqrt{1 + 8n^2}}{4n} \right)^4 \right] V_{\Sigma}. \quad (3.17)$$

The Rényi entropies  $S_n$  as a function of  $n$  can be easily generalized to higher dimensions, based on the solution of hyperbolic black holes with scalar hair in AdS <sub>$d+1$</sub> ; see [24] for details of this solution. The Rényi entropies calculated from the hairy black holes are

$$S_n = \frac{nL^{d-1}}{8(n-1)G} \left[ 2 - \mathcal{S}_{\pm}(\alpha, n)^{a/c} - \mathcal{S}_{\pm}(\alpha, n)^{b/c} \right] V_{\Sigma}, \quad (3.18)$$

where

$$\mathcal{S}_{\pm}(\alpha, n) = \frac{1}{bn} \left( c \pm \sqrt{c^2 + abn^2} \right), \quad (3.19)$$

$$\begin{cases} \mathbf{a} = 2(d-2)^2 - d(d-1)\alpha^2, \\ \mathbf{b} = (d-2)[2d - (d-1)\alpha^2], \\ \mathbf{c} = 2(d-2) + (d-1)\alpha^2. \end{cases} \quad (3.20)$$

With phase transitions, the Rényi entropies  $\bar{S}_n$  is non-analytic at  $n$  corresponding to the phase transition temperature of the black holes,  $T = T_0/n = (2\pi Ln)^{-1}$ . When  $0 < \alpha \leq (d-2)\sqrt{\frac{2}{d(d-1)}}$  and  $\alpha \geq \sqrt{\frac{2d}{(d-1)}}$ , the Rényi entropies  $\bar{S}_n$  are given by (2.14), in which  $S_n$  is (3.18). When  $(d-2)\sqrt{\frac{2}{d(d-1)}} < \alpha < \sqrt{\frac{2d}{(d-1)}}$ , the Rényi entropies  $\bar{S}_n$  are given by (2.15) with the critical parameter  $n_m$  determined by the minimum temperature. A zeroth-order phase transition occurs at the minimum temperature

$$T_m = \frac{\sqrt{-ab}}{2\pi cL}, \quad (3.21)$$

or equivalently,

$$n_m = \frac{T_0}{T_m} = \frac{c}{\sqrt{-ab}}. \quad (3.22)$$

We can consider a variant of the Rényi entropy used in [28],

$$\tilde{S}_n \equiv n^2 \partial_n \left( \frac{n-1}{n} S_n \right) = \frac{L^2}{4G} \mathcal{S}_{\pm}(\alpha, n)^{\frac{a+b}{2c}} V_{\Sigma}, \quad (3.23)$$

which satisfies an area law and equals the thermal entropy of the hyperbolic black hole.

## 4 Entanglement spectrum

The entanglement spectrum is the eigenvalue distribution of the reduced density matrix. With the Rényi entropies of all orders, the entanglement spectrum is determined. Generally, the spectrum should include both discrete and continuous parts [12]. We briefly review the analysis. Assuming that the eigenvalue distribution is discrete, we can write the Rényi entropies as

$$S_n = \frac{1}{1-n} \log \text{Tr}[\rho^n] = \frac{1}{1-n} \log \left( \sum_i d_i \lambda_i^n \right), \quad (4.1)$$

where  $\lambda_i$  are the eigenvalues of the reduced density matrix satisfying  $\lambda_1 > \lambda_2 > \dots$ , and  $d_i$  is the degeneracy of  $\lambda_i$ . The large  $n$  expansion of (4.1) gives

$$S_n = -\log \lambda_1 - \frac{1}{n} \log(d_1 \lambda_1) + \mathcal{O} \left[ \frac{1}{n^2}, \frac{1}{n} \left( \frac{\lambda_2}{\lambda_1} \right)^n \right], \quad (4.2)$$

where the last term leads to non-analyticity in  $1/n$ . A continuous spectrum will also lead to non-analyticity. However, the holographic calculations in sections 2 and 3 do not show any non-analyticity in  $1/n$ , and thus the spectrum should include both discrete and continuous parts. Furthermore, from the thermal perspective of the dual CFT, the analyticity

allows only one discrete eigenvalue  $\lambda_1$ , which is also the largest eigenvalue of the continuous spectrum [12].

In terms of the analysis above, the Rényi entropies can be written as

$$S_n = \frac{1}{1-n} \log \left[ d_1 \lambda_1^n + \int_0^{\lambda_1} \bar{\rho}(\lambda) \lambda^n d\lambda \right], \quad (4.3)$$

where  $\bar{\rho}(\lambda)$  is the continuous part of the entanglement spectrum  $\rho(\lambda)$ . Moreover,  $\bar{\rho}(\lambda)$  is analytic at  $\lambda = \lambda_1$ , and we can write the discrete part of  $\rho(\lambda)$  as a Dirac delta function. Thus, the Rényi entropies satisfy

$$\exp[(1-n)S_n] = \int_{t_1}^{+\infty} e^{-(n+1)t} \rho(e^{-t}) dt, \quad (4.4)$$

where  $\lambda$  is reparameterized as  $\lambda = e^{-t}$ , and  $\lambda_1 = e^{-t_1}$ . The lower limit of the integral (4.4) can be changed to zero, which gives nothing but the Laplace transform. Thus, the spectrum can be derived from an inverse Laplace transform with  $n$  as the parameter,

$$\rho(\lambda) = \frac{1}{\lambda} \mathcal{L}^{-1} [e^{(1-n)S_n}, n, t] \Big|_{t=-\log \lambda} = \frac{1}{\lambda} \frac{1}{2\pi i} \lim_{T \rightarrow \infty} \int_{\gamma-iT}^{\gamma+iT} e^{(1-n)S_n} e^{nt} dn, \quad (4.5)$$

where the integral is taken over a vertical line with  $\text{Re}(s) = \gamma$ , and  $\gamma$  is a real number ensuring no singularity on the right side of this line.

In condensed matter literature, people are more interested in the low-lying part<sup>8</sup> of the entanglement spectrum, which implies more universal properties of the system [4, 11]. Especially in  $(1+1)$  dimensions, the strong conformal invariance fixes the continuous spectrum entirely, so the universal information beyond the entanglement entropy is embodied in the location and degeneracies of the low-lying eigenvalues [11]. However, the cases in higher dimensions imply more complex properties. The systems corresponding to different  $\alpha$  have different continuous spectra as well as discrete parts.

Note that the entanglement spectrum depends on all  $n$  including the  $n < 1$  part. It is difficult to perform the inverse Laplace transform for the Rényi entropies  $\bar{S}_n$  with phase transitions. Instead, we use the analytic solution of the Rényi entropies  $S_n$  calculated from hyperbolic black holes with scalar hair, and explicitly obtain the entanglement spectrum as an infinite sum. We show that the low-lying part of the entanglement spectrum is determined by the large  $n$  behavior of the Rényi entropies, and briefly discuss the effects of phase transitions.

#### 4.1 Entanglement spectrum from AdS<sub>4</sub> black holes

We start with special cases when  $\alpha = 1/\sqrt{3}$  or  $\sqrt{3}$ , from which the spectrum can be derived straightforwardly. The Rényi entropies have a simple form

$$S_n = \frac{L^2}{8G} \left( 1 + \frac{1}{n} \right) V_\Sigma. \quad (4.6)$$

---

<sup>8</sup>Following [4], we use the term low-lying, which represents the spectrum with lower energy, or with  $\lambda$  closer to the largest eigenvalue.



This result has the same  $n$  dependence as the universal result (2.21) in 2D CFTs, whose entanglement spectrum can be calculated by means of properties of the polylogarithm function [11] or Mellin's inversion formula [35]:

$$\rho(\lambda) = \delta(\lambda_1 - \lambda) + \frac{b\theta(\lambda_1 - \lambda)}{\lambda\sqrt{b\ln(\lambda_1/\lambda)}} I_1(2\sqrt{b\ln(\lambda_1/\lambda)}), \quad (4.7)$$

with

$$b = -\ln \lambda_1 = \frac{L^2}{8G} V_\Sigma, \quad (4.8)$$

where  $I_k(x)$  is the modified Bessel function of the first kind and  $\theta(x)$  is the Heaviside step function.

In general cases, we can still calculate the entanglement spectrum in terms of an infinite sum if the Rényi entropies are analytic at  $n = \infty$ . This analyticity allows us to expand the Rényi entropies near  $n = \infty$  as

$$S_n = \sum_{i=0}^{\infty} s_i n^{-i}, \quad (4.9)$$

where the coefficients of the first two terms are<sup>9</sup>

$$\begin{aligned} s_0 &= \frac{L^2}{4G} \left( 1 - 2|1 - \alpha^2| \cdot |1 - 3\alpha^2|^{\frac{1-3\alpha^2}{2(1+\alpha^2)}} |3 - \alpha^2|^{\frac{\alpha^2-3}{2(1+\alpha^2)}} \right) V_\Sigma, \\ s_1 &= s_0 - \frac{L^2}{4G} \left( \frac{1 - 3\alpha^2}{3 - \alpha^2} \right)^{\frac{1-\alpha^2}{1+\alpha^2}} V_\Sigma, \end{aligned} \quad (4.10)$$

whose limits at  $\alpha = 1/\sqrt{3}$  and  $\sqrt{3}$  are

$$s_0 = s_1 = \frac{L^2}{8G} V_\Sigma. \quad (4.11)$$

By the approach in [13], the inverse Laplace transform of the LHS of (4.4) can be calculated by writing it as an infinite sum. Here we give more analytic details together with our explicit expression of  $S_n$ . We expand the LHS of (4.4) as

$$\begin{aligned} \exp[(1-n)S_n] &= \exp(s_0 - s_1 - s_0 n) \exp\left(\sum_{i=1}^{\infty} u_i n^{-i}\right) \\ &= \left(1 + \sum_{i=1}^{\infty} v_i n^{-i}\right) \exp(s_0 - s_1 - s_0 n), \end{aligned} \quad (4.12)$$

where  $u_i$  and  $v_i$  can be written as the function of expansion coefficients of  $S_n$ , i.e.,

$$u_i = s_i - s_{i+1}, \quad v_i = \frac{1}{i!} B_i(u_1, 2!u_2, \dots, i!u_i), \quad (4.13)$$

where  $B_i$  are the complete exponential Bell polynomials, which can be expressed as an infinite sum (see appendix B for details).

<sup>9</sup>They are obtained by expanding (2.12), which is well defined at  $n \rightarrow \infty$  when  $0 \leq \alpha \leq 1/\sqrt{3}$  or  $\alpha \geq \sqrt{3}$ . When  $1/\sqrt{3} < \alpha < \sqrt{3}$ , the  $n \rightarrow \infty$  behavior of the Rényi entropies is determined by the SAdS black hole ( $\alpha = 0$ ) due to the zeroth-order phase transition of the hyperbolic black holes.

The inverse Laplace transform of (4.12) is given by the convolution theorem

$$\begin{aligned}\rho(\lambda) &= \frac{\exp(s_0 - s_1)}{\lambda} \left( \lambda_1 \delta(\lambda_1 - \lambda) + \sum_{i=0}^{\infty} \frac{v_{i+1}}{i!} (\ln(\lambda_1/\lambda))^i \theta(\lambda_1 - \lambda) \right) \\ &= \exp(s_0 - s_1) \left( \delta(\lambda_1 - \lambda) + \frac{\theta(\lambda_1 - \lambda)}{\lambda} \sum_{i=0}^{\infty} \frac{v_{i+1}}{i!} (\ln(\lambda_1/\lambda))^i \right).\end{aligned}\quad (4.14)$$

Similar to the special case (4.7), the general spectrum also includes a Dirac delta function and Heaviside step function determined by the largest eigenvalue  $\lambda_1$ , which provides an example to verify the analysis above that the spectrum consists of one discrete eigenvalue and the continuous part. The largest eigenvalue of the spectrum is given by the constant term of the Rényi entropies

$$\begin{aligned}\lambda_1 &= \exp(-s_0) \\ &= \begin{cases} \exp\left[\frac{L^2}{4G} (2|1 - \alpha^2| \cdot |1 - 3\alpha^2|^{\frac{1-3\alpha^2}{2(1+\alpha^2)}} |3 - \alpha^2|^{\frac{\alpha^2-3}{2(1+\alpha^2)}} - 1) V_\Sigma\right], & 0 \leq \alpha \leq 1/\sqrt{3} \text{ or } \alpha \geq \sqrt{3}, \\ \exp\left[\frac{L^2}{36G} (2\sqrt{3} - 9) V_\Sigma\right], & 1/\sqrt{3} < \alpha < \sqrt{3}. \end{cases}\end{aligned}\quad (4.15)$$

By comparing (4.14) with the ansatz (4.3), the degeneracy of the eigenvalue  $\lambda_1$  is

$$d_1 = \exp(s_0 - s_1) = \begin{cases} \exp\left[\frac{L^2}{4G} \left(\frac{1-3\alpha^2}{3-\alpha^2}\right)^{\frac{1-\alpha^2}{1+\alpha^2}} V_\Sigma\right], & 0 \leq \alpha \leq 1/\sqrt{3} \text{ or } \alpha \geq \sqrt{3}, \\ \exp\left(\frac{L^2}{12G} V_\Sigma\right), & 1/\sqrt{3} < \alpha < \sqrt{3}, \end{cases}\quad (4.16)$$

which reduces to  $d_1 = 1$  when  $\alpha = 1/\sqrt{3}$  and  $\sqrt{3}$ . The above calculations show that the largest eigenvalue of the entanglement spectrum decreases while its degeneracy increases if we enlarge the entangling sphere. Besides, the density of the continuous part  $\bar{\rho}(\lambda)$  increases. The normalization of the spectrum (4.14) can be verified numerically to satisfy

$$d_1 \lambda_1 + \int_0^{\lambda_1} \lambda \bar{\rho}(\lambda) d\lambda = 1.\quad (4.17)$$

As a special example, when  $\alpha = 1/\sqrt{3}$  or  $\sqrt{3}$ , we have  $s_0 = s_1$  and  $s_i = 0$  ( $i > 1$ ). Inserting them into (4.13) and (4.14), we obtain the spectrum

$$\begin{aligned}\rho(\lambda) &= \delta(\lambda_1 - \lambda) + \frac{1}{\lambda} \sum_{i=0}^{\infty} \frac{s_0^{i+1}}{i!(i+1)!} (\ln(\lambda_1/\lambda))^i \theta(\lambda_1 - \lambda) \\ &= \delta(\lambda_1 - \lambda) + \frac{s_0 \theta(\lambda_1 - \lambda)}{\lambda \sqrt{s_0 \ln(\lambda_1/\lambda)}} I_1(2\sqrt{s_0 \ln(\lambda_1/\lambda)}),\end{aligned}\quad (4.18)$$

which exactly gives the result (4.7). For general cases, the entanglement spectrum is shown in figures 4 and 5. The spectrum in AdS<sub>5</sub> is the same as (4.18) when  $\alpha = 2/\sqrt{6}$  or  $4/\sqrt{6}$ .

We note that the expansion of the Rényi entropies at  $n = \infty$  (4.9) has a radius of convergence. From (2.12) and (2.13), the expansion converges for  $n$  larger than a special value  $n_c$  determined by  $\alpha$  ( $0 \leq \alpha \leq 1/\sqrt{3}$  and  $\alpha \geq \sqrt{3}$ ),

$$n_c = \frac{1 + \alpha^2}{\sqrt{(3 - \alpha^2)(1 - 3\alpha^2)}},\quad (4.19)$$

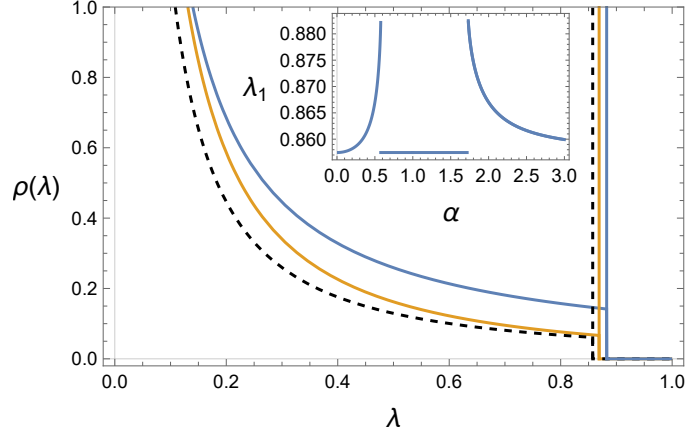


**Figure 4.** The entanglement spectrum as a function of  $\lambda$ . The dashed line is for the SAdS<sub>4</sub> black hole, while the solid lines are for hairy black holes, with  $\alpha = 0.52$  (orange line) and  $1/\sqrt{3}$  or  $\sqrt{3}$  (blue line). The largest eigenvalues are 0.857, 0.869, 0.882, respectively. The largest eigenvalue as a function of  $\alpha$  is shown in the subfigure.

which increases as  $\alpha$  approaches  $1/\sqrt{3}$  or  $\sqrt{3}$ . When  $\alpha \leq \sqrt{2} - 1$  or  $\alpha \geq \sqrt{2} + 1$ , the expansion can converge at  $n = 1$ . Therefore, we shall not expect the expansion (4.9) to describe the Rényi entropies of all orders, especially when  $\alpha$  is extremely close to  $1/\sqrt{3}$  or  $\sqrt{3}$ . This leads to non-commutativity of the  $\alpha \rightarrow 1/\sqrt{3}$  and  $n \rightarrow \infty$  limits of the Rényi entropies. As long as  $\alpha$  is not too close to  $1/\sqrt{3}$  or  $\sqrt{3}$ , the spectrum given by the series (4.14) is expected to explicitly describe the low-lying part (larger  $\lambda$ ), which is determined by the large  $n$  behavior of the Rényi entropies. The spectrum for  $\lambda$  close to zero may be inconsistent with (4.14), and needs to be treated differently.

For  $\lambda \rightarrow 0$ , the spectrum can be approximated by the saddle point method. The saddle point  $n_0$  is given by

$$\frac{\partial}{\partial n} ((n-1)S_n) \Big|_{n_0} + \ln \lambda = 0, \quad (4.20)$$

and the integral (4.5) is approximated as

$$\rho(\lambda \rightarrow 0) \sim \frac{1}{\lambda^{n+1}} e^{(1-n)S_n} \left[ 2\pi \frac{\partial^2}{\partial n^2} ((1-n)S_n) \right]^{-1/2} \Big|_{n_0}. \quad (4.21)$$

For instance, the saddle point is  $n_0 = \sqrt{s_0 / \ln(\lambda_1/\lambda)}$  when  $\alpha = 1/\sqrt{3}$ . The consistency is convenient to verify by changing the variable  $t = -\ln \lambda$

$$\rho(t \rightarrow \infty) \sim \frac{1}{16\sqrt{\pi}} [s_0(t-s_0)]^{-3/4} e^{2\sqrt{s_0(t-s_0)}}, \quad (4.22)$$

which gives the leading term of the asymptotic expansion of (4.18) at  $t = \infty$ . Considering the phase transition at  $n = 1$ , all these spectra should have the same  $\lambda \rightarrow 0$  behavior (as the SAdS solution), whose saddle point is  $n_0 = (2/t)^{1/3}/3 + \mathcal{O}(t^{-4/3})$ .

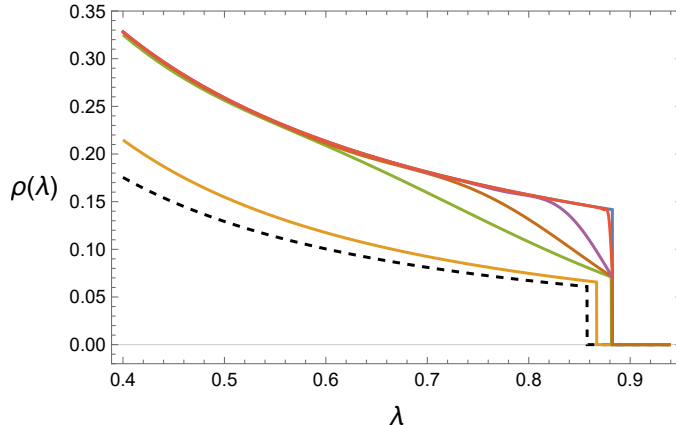


**Figure 5.** The entanglement spectrum near  $\alpha = 1/\sqrt{3}$ . The dashed line is for the SAdS<sub>4</sub> black hole, while the solid lines are for hairy black holes, where the yellow, green, brown, purple, red, and blue lines are for  $\alpha = 0.5, 0.576, 0.577, 0.5773, 0.57735,$  and  $1/\sqrt{3}$ , respectively. Here we plot only the continuous spectrum.

As a comparison, we also employ numerical methods<sup>10</sup> to evaluate the inverse Laplace transform, which shows that the spectrum obtained from (4.14) is accurate for a wide range of  $\lambda$  as long as  $\alpha$  is not extremely close to  $1/\sqrt{3}$ . Therefore, the series (4.14) is sufficient to describe the low-lying entanglement spectrum, except when  $\alpha$  is extremely close to  $1/\sqrt{3}$  (or  $\sqrt{3}$ ). The low-lying spectrum for  $\alpha$  close to  $1/\sqrt{3}$  is plotted in figure 5 numerically, from which we can see the spectrum has unique behavior when  $\lambda$  approaches  $\lambda_1$ :

- When  $\alpha$  is not extremely close to  $1/\sqrt{3}$ , the spectrum gradually changes with respect to  $\alpha$  as a whole, and the largest eigenvalue increases, as expected.
- When  $\alpha$  is extremely close to  $1/\sqrt{3}$ , the continuous part of the spectrum near  $\lambda_1$  experiences dramatical change: the spectral density of large eigenvalues increases with  $\alpha$ , while the spectrum with small eigenvalues is almost fixed. The degeneracy of  $\lambda_1$  decreases while the location keeps almost fixed.

In the procedure from (4.9) to (4.14), we neglect the third-order phase transition of the Rényi entropies because the spectrum of the low-lying part is not affected by the phase transition at  $n = 1$ , based on the following observations. First, the spectrum near the largest eigenvalue  $\lambda_1$  is entirely determined by the large  $n$  behavior of the Rényi entropies. Second, the saddle point approximation shows that the spectrum with  $\lambda \rightarrow 0$  is dominated by the Rényi entropies with  $n \rightarrow 0$ . Furthermore, when we perform the expansion (4.9) and (4.12), we find that the number of terms and the precision of the expansion would significantly affect the Rényi entropies (4.9) beyond the convergent region. However, the spectrum obtained from these expansions does not show any difference for a wide range of  $\lambda$ .

<sup>10</sup>Some details of numerical methods are given in [36] (or see appendix B). Different methods can give different results, some of which are unreliable in our cases. Because of the great change when  $\alpha$  approaches  $1/\sqrt{3}$ , a singularity of (2.12), we test the accuracy of numerical methods by comparing the cases when  $\alpha$  is extremely close to  $1/\sqrt{3}$  with (4.7), shown in figure 5.

Another similar observation comes from the comparison between some numerical methods and (4.14), which shows consistency until  $\lambda$  is small enough (near zero). These observations suggest that the spectrum of different  $\lambda$  is affected by different parts of the Rényi entropies: the spectrum with large  $\lambda$  is not significantly affected by small  $n$ . As a consequence, the phase transition at  $n = 1$  is merely embodied in the spectrum with  $\lambda$  close to zero, and the spectra for different  $\alpha$  have the same asymptotic behavior (as the SAdS black hole) at  $\lambda \rightarrow 0$ .

Besides the phase transition at  $n = 1$  where  $\partial_n^2 \bar{S}_n$  is discontinuous, a zeroth-order phase transition exists for  $1/\sqrt{3} < \alpha < \sqrt{3}$  ( $\alpha \neq 1$ ) at  $n = n_m$  where  $\bar{S}_n$  is discontinuous; see figure 2. The approximation (4.20) implies another saddle point  $n_m$ . So the  $\lambda \rightarrow 0$  behavior of the entanglement spectrum may be different from the SAdS one, although they have the same  $n \rightarrow 0$  behavior of the Rényi entropies. However, due to the same large  $n$  behavior of the Rényi entropies, the spectrum near  $\lambda_1$  should be the same as the SAdS case if  $\alpha$  is not extremely close to  $1/\sqrt{3}$  or  $\sqrt{3}$ . It would be interesting to see how the phase transitions affect the full entanglement spectrum more precisely.

## 5 Summary and discussion

In this paper, we have calculated the Rényi entropies (with a spherical entangling surface) and entanglement spectrum from a class of hyperbolic black holes with scalar hair in terms of the conformal mapping approach [12, 18]. The main conclusions are as follows:

- By employing a class of hyperbolic black holes with scalar hair as a one-parameter family generalization of the MTZ black hole, we explicitly obtain the holographic Rényi entropies. The  $n \rightarrow 1$  limit of these Rényi entropies gives the same entanglement entropy, while the Rényi entropies with  $n > 1$  are affected by the scalar field. In special cases when  $\alpha = 1/\sqrt{3}$  or  $\sqrt{3}$  (in AdS<sub>4</sub>) and  $\alpha = 2/\sqrt{6}$  or  $4/\sqrt{6}$  (in AdS<sub>5</sub>), which correspond to special cases of STU supergravity, the Rényi entropies have the same  $n$  dependence as the universal result in 2D CFTs.
- The zeroth-order and third-order phase transitions of black holes lead to the discontinuity of the Rényi entropies and their second derivatives at special values  $n_m$ , which depend on the phase transition temperature of black holes.
- From the Rényi entropies that are analytic at  $n = \infty$ , we calculate the entanglement spectrum as an infinite sum by means of the exponential Bell polynomials. The result includes a Dirac delta function and a Heaviside step function determined by the large  $n$  limit of the Rényi entropies. This approach is verified to be accurate for a wide range of eigenvalues by comparing it with numerical calculations. We take a closer look at the spectrum when  $\alpha$  is extremely close to  $1/\sqrt{3}$  (in AdS<sub>4</sub>), which shows different properties.

The following topics need further investigation: (i) It would be intriguing to explicitly show how phase transitions are embodied in the entanglement spectrum. (ii) This work

focuses on the neutral limit, while the charged hyperbolic black holes include more complex phase structures and are worth investigating. (iii) In special cases that intersect with STU supergravity, it would be interesting to compare our work with the supersymmetric Rényi entropies studied in [37].

## Acknowledgments

We thank Yi Wang for helpful conversations. This work was supported in part by the NSF of China under Grant No. 11905298 and the Undergraduate Base Scientific Research Project under Grant No. 20211222.

## A Black hole thermodynamics with generalized boundary condition

Since the thermodynamics of the hyperbolic black holes plays a key role in calculating the Rényi entropies, we study the holographic renormalization of the black holes with scalar hair by giving the boundary counter terms and generalized boundary conditions.

The free energy of a black hole is calculated from the renormalized on-shell action with proper boundary counter terms. For our Einstein-scalar system in AdS<sub>4</sub> with  $m^2 L^2 = -2$ , we consider the following boundary terms<sup>11</sup>

$$S_{\partial} = \frac{1}{16\pi G} \int d^3x \sqrt{-\gamma} \left( 2K - \frac{4}{L} - LR[\gamma] - \frac{1}{2L} \phi^2 - \frac{W(\phi_a)}{L\phi_a^3} \phi^3 \right), \quad (\text{A.1})$$

where  $\gamma_{\mu\nu}$  is the induced metric,  $K$  is the extrinsic curvature calculated from the unit normal vector pointing out of the AdS boundary, and  $\phi_a$  is a coefficient in (A.14) below. The first term being the Gibbons-Hawking boundary term for a well-defined Dirichlet variational problem and the following three terms remove the divergence in the bulk action. The last term of (A.1) is a finite boundary term [39]. We set the AdS radius  $L = 1$  in the following. By variation of the action with respect to the induced metric  $\gamma_{\mu\nu}$ , we obtain the boundary stress tensor

$$\langle T_{\mu\nu} \rangle = \frac{1}{16\pi G} \lim_{z \rightarrow 0} z^{-1} \left[ 2(Kh_{\mu\nu} - K_{\mu\nu} - 2h_{\mu\nu} + G_{\mu\nu}) - \left( \frac{1}{2} \phi^2 + \frac{W(\phi_a)}{\phi_a^3} \phi^3 \right) h_{\mu\nu} \right], \quad (\text{A.2})$$

where  $z$  is the AdS radial coordinate in (A.3) below, and  $G_{\mu\nu}$  is the Einstein tensor calculated from  $\gamma_{\mu\nu}$ .

We formulate the first law of thermodynamics without imposing a boundary condition, and then show that the first law of thermodynamics is unmodified by a scalar charge with a generalized boundary condition  $\phi_b = W'(\phi_a)$ , whose special cases correspond to multi-trace deformations in the dual CFT. We will follow the procedure in [40] with a generalization for imposing boundary conditions of the scalar field. The choice  $W(\phi_a) = c\phi_a^3$  ( $c$  is a constant) gives the same result as in [40].

---

<sup>11</sup>We obtain exactly the same renormalized on-shell action as in [26, 38], although the expressions of the boundary terms are slightly different.

For convenience of numerical calculations, and to see the difference between planar and hyperbolic/spherical black holes, we use the metric ansatz

$$ds^2 = \frac{1}{z^2} \left( -g(z)e^{-\chi(z)} dt^2 + \frac{dz^2}{g(z)} + d\Sigma_{2,k}^2 \right), \quad (\text{A.3})$$

where  $k = 0, -1, 1$  are for planar, hyperbolic, and spherical black holes, respectively. In practice, we can write  $d\Sigma_{2,k}^2$  as

$$d\Sigma_{2,k}^2 = \frac{dx^2}{1 - kx^2} + (1 - kx^2)d\varphi^2. \quad (\text{A.4})$$

The AdS boundary is at  $z = 0$ , and the horizon is at  $z = z_h$ . Unlike the  $k = 0$  case in which  $z_h$  can be fixed to be  $z_h = 1$  by scaling symmetries,  $z_h$  is an extra parameter when  $k \neq 0$ . The equations of motion for the metric and the scalar field are

$$g' - \left( \frac{\chi'}{2} + \frac{3}{z} \right) g - \frac{1}{2z} V(\phi) + kz = 0, \quad (\text{A.5})$$

$$\chi' - \frac{1}{2} z \phi'^2 = 0, \quad (\text{A.6})$$

$$\phi'' + \left( \frac{g'}{g} - \frac{\chi'}{2} - \frac{2}{z} \right) \phi' - \frac{1}{z^2} V'(\phi) = 0. \quad (\text{A.7})$$

Near the horizon  $z = z_h$ , the asymptotic behavior of the functions is

$$g = \bar{g}_1(z_h - z) + \bar{g}_2(z_h - z)^2 + \dots, \quad (\text{A.8})$$

$$\chi = \chi_h + \bar{\chi}_1(z_h - z) + \dots, \quad (\text{A.9})$$

$$\phi = \phi_h + \bar{\phi}_1(z_h - z) + \dots, \quad (\text{A.10})$$

where  $\chi_h$  and  $\phi_h$  can be used to express other coefficients. The temperature and entropy density are given by

$$T = \frac{\bar{g}_1 e^{-\chi_h/2}}{4\pi}, \quad s = \frac{1}{4Gz_h^2}. \quad (\text{A.11})$$

Near the AdS boundary  $z = 0$ , the asymptotic behavior of the functions is

$$g = 1 + \left( k + \frac{1}{4} \phi_a^2 \right) z^2 + g_3 z^3 + \dots, \quad (\text{A.12})$$

$$e^{-\chi} g = 1 + kz^2 + \left( g_3 - \frac{2}{3} \phi_a \phi_b \right) z^3 + \dots, \quad (\text{A.13})$$

$$\phi = \phi_a z + \phi_b z^2 + \dots, \quad (\text{A.14})$$

where higher-order coefficients generally depend on the specific potential  $V(\phi)$ . By substituting the boundary expansions into (A.2), we obtain the stress tensor. Let  $\langle T^\mu_\nu \rangle = \text{diag}(-\varepsilon, p, p, p)$ , and we have

$$\varepsilon = \frac{1}{16\pi G} (-2g_3 + \phi_a \phi_b + W(\phi_a)), \quad (\text{A.15})$$

$$p = \frac{1}{16\pi G} (-g_3 + \phi_a \phi_b - W(\phi_a)), \quad (\text{A.16})$$

where  $\varepsilon$  is the energy density and  $p$  is the pressure density. The trace of the stress tensor is

$$\langle T^\mu{}_\mu \rangle = -\varepsilon + 2p = \frac{1}{16\pi G} (\phi_a \phi_b - 3W(\phi_a)). \quad (\text{A.17})$$

We adopt a general procedure developed by Wald [41] to formulate the first law of black hole thermodynamics. By variation of parameters in a  $(d+1)$ -dimensional solution, there is a closed  $(d-1)$ -form  $\delta Q - i_\xi \Theta$  with  $\xi$  being a Killing vector. Here we take  $\xi = \partial/\partial t$ . Thus, the variation of a Hamiltonian is defined by the integral

$$\delta H = \int_{\Sigma^{(d-1)}} (\delta Q - i_\xi \Theta), \quad (\text{A.18})$$

where  $\Sigma^{(d-1)}$  is a  $(d-1)$ -dimensional surface at constant  $t$  and  $z$ . A key observation in [41] is that  $\delta H$  is a radially conserved quantity, i.e.,  $\delta H$  is independent of  $z$ , and takes the same value at the horizon and the AdS boundary. For the construction of  $\delta H$  in Einstein-scalar systems, see [42, 43].

For the Einstein-scalar system (2.1) with the metric (A.3),  $\delta H$  at radius  $z$  is given by

$$\delta H = -\frac{V_\Sigma}{16\pi G} z^{-2} e^{-\chi/2} \left( \frac{2}{z} \delta g - g \phi' \delta \phi \right), \quad (\text{A.19})$$

where  $V_\Sigma$  is the volume of  $d\Sigma_{2,k}^2$ . First we evaluate  $\delta H$  at the horizon. From (A.8), we have  $\delta g|_{z=z_h} = \bar{g}_1 \delta z_h$ , and we obtain

$$\frac{\delta H}{V_\Sigma} \Big|_{z=z_h} = -\frac{1}{8\pi G} e^{-\chi(z_h)/2} \bar{g}_1 z_h^{-3} \delta z_h = T \delta s, \quad (\text{A.20})$$

where we have used  $\delta s = \delta(1/(4Gz_h^2)) = -1/(2Gz_h^3) \delta z_h$ . Evaluating  $\delta H$  at the AdS boundary gives

$$\frac{\delta H}{V_\Sigma} \Big|_{z=0} = -\frac{1}{16\pi G} \lim_{z \rightarrow 0} z^{-2} e^{-\chi/2} \left( \frac{2}{z} \delta g - g \phi' \delta \phi \right) = \frac{1}{16\pi G} (-2\delta g_3 + \phi_a \delta \phi_b + 2\phi_b \delta \phi_a). \quad (\text{A.21})$$

The variation of the energy density (A.15) gives

$$\delta \varepsilon = \frac{1}{16\pi G} (-2\delta g_3 + \phi_a \delta \phi_b + (\phi_b + W'(\phi_a)) \delta \phi_a). \quad (\text{A.22})$$

Then we obtain

$$\frac{\delta H}{V_\Sigma} \Big|_{z=0} = \delta \varepsilon + \frac{1}{16\pi G} (\phi_b - W'(\phi_a)) \delta \phi_a. \quad (\text{A.23})$$

We will set  $16\pi G = 1$  for simplicity. By equating  $\delta H$  at the horizon and the boundary, we obtain the first law of thermodynamics:

$$\delta \varepsilon = T \delta s - (\phi_b - W'(\phi_a)) \delta \phi_a. \quad (\text{A.24})$$

We can clearly see that upon imposing a generalized boundary condition  $\phi_b = W'(\phi_a)$ , the first law of thermodynamics is unmodified by the scalar field.

In other words, for a boundary condition parametrized by  $\phi_b = W'(\phi_a)$ , we can always formulate the first law of thermodynamics  $d\varepsilon = T ds$  (unmodified by a scalar charge) if we



choose the boundary terms (A.1). Special cases include multi-trace deformations of the dual CFT. The double-trace deformation corresponds to  $\phi_b/\phi_a = \kappa$ , and thus  $W(\phi_a) = (1/2)\kappa\phi_a^2$ . The triple-trace deformation corresponds to  $\phi_b/\phi_a^2 = \tau$ , and thus  $W(\phi_a) = (1/3)\tau\phi_a^3$ .

The free energy is calculated by the renormalized on-shell action as  $F/T = -(S + S_\partial)$ , where  $S$  is the bulk action and  $S_\partial$  is the boundary counter terms. The free energy density is the free energy per volume:  $f = F/V_\Sigma$ . Evaluating the bulk action gives

$$-S = \int d^3x \int_{z_h}^0 dz \left[ \left( \frac{2}{z^3} g e^{-\chi/2} \right)' + 2kz^{-2} e^{-\chi/2} \right] \quad (\text{A.25})$$

$$= T^{-1} V_\Sigma \frac{2}{z^3} g e^{-\chi/2} \Big|_{z=0} + 2kT^{-1} V_\Sigma \int_{z_h}^0 z^{-2} e^{-\chi/2} dz. \quad (\text{A.26})$$

When  $k = 0$ , the bulk Lagrangian is a total derivative [44], and thus we can express the action in terms of boundary quantities. When  $k \neq 0$ , however, the action will inevitably involve an integral from the horizon to the boundary. Consequently, the free energy density is given by

$$f = \underbrace{g_3 - \phi_a \phi_b + W(\phi_a)}_{-p} + 2k \left( \frac{1}{z} + \int_{z_h}^z \bar{z}^{-2} e^{-\chi(\bar{z})/2} d\bar{z} \right) \Big|_{z=0}. \quad (\text{A.27})$$

We can verify that the thermodynamic relation  $f = \varepsilon - Ts$  is satisfied by using a radially conserved quantity [45]

$$\begin{aligned} \mathcal{Q} &= z^{-2} e^{\chi/2} (g e^{-\chi})' + 2k \int z^{-2} e^{-\chi/2} dz \\ &\equiv z^{-2} e^{\chi/2} (g e^{-\chi})' + 2k \mathcal{P}(z), \end{aligned} \quad (\text{A.28})$$

which satisfies  $\mathcal{Q}'(z) = 0$ . Evaluating  $\mathcal{Q}$  at the horizon gives

$$\mathcal{Q}|_{z=z_h} = -Ts + 2k\mathcal{P}(z_h). \quad (\text{A.29})$$

Evaluating  $\mathcal{Q}$  at the AdS boundary gives

$$\mathcal{Q}|_{z=0} = \underbrace{3g_3 - 2\phi_a \phi_b}_{-(\varepsilon + p)} + 2k \left( \frac{1}{z} + \mathcal{P}(z) \right) \Big|_{z=0}, \quad (\text{A.30})$$

where we have used (A.15) and (A.16). By equating (A.29) and (A.30), we obtain the free energy density  $f = \varepsilon - Ts$ , which is exactly the same as (A.27). We can see that when  $k = 0$ , we have  $f = -p$ . For hyperbolic/spherical black holes, in contrast, the free energy depends on a bulk integral. Nevertheless, the first law of thermodynamics is valid for all  $k$ . We have  $df = -sdT$  for the boundary condition  $\phi_b = W'(\phi_a)$  together with the boundary terms (A.1).

With the analytic solution in hand, we can verify the first law of thermodynamics with the boundary condition given by a triple-trace deformation. For the boundary condition given by a double-trace deformation, we can numerically solve the Einstein-scalar

system (2.1) with the potential (2.2) by the numerical techniques described in [44]. Integrating out from the horizon to the AdS boundary gives a map

$$(z_h, \phi_h) \mapsto (\phi_a, \phi_b, g_3). \quad (\text{A.31})$$

Upon imposing the boundary condition  $\phi_b = \kappa\phi_a$ , we obtain a two-parameter family of solutions, where the two parameters are two dimensionless combinations of  $(z_h, T, \kappa)$ . By extracting the thermodynamic quantities  $\varepsilon$ ,  $T$ , and  $s$  from the numerical solution, we have verified that the first law of thermodynamics  $d\varepsilon = Tds$  is satisfied.

## B Mathematical notes

### B.1 Inverse Laplace transform

The Laplace transform of a real variable function  $f(t)$  is defined as

$$F(s) = \mathcal{L}[f(t)](s) = \int_0^\infty f(t)e^{-st} dt. \quad (\text{B.1})$$

The inverse Laplace transform can be obtained by Mellin's inversion formula

$$f(t) = \mathcal{L}^{-1}[F(s)](t) = \frac{1}{2\pi i} \lim_{T \rightarrow \infty} \int_{\gamma-iT}^{\gamma+iT} F(s)e^{st} dt = \sum_{i=1} \text{Res}[e^{st}F(s), s_i], \quad (\text{B.2})$$

where the integral is taken over a vertical line with  $\text{Re}(s) = \gamma$ , and  $\gamma$  is a real number ensuring no singularities on the right side of this line. Thus the result can be obtained by considering the residues of  $e^{st}F(s)$  at all isolated singularities  $s_i$  on the complex plane. Two basic inversions related to our calculations are

$$\mathcal{L}^{-1}[e^{-\tau s}](t) = \delta(t - \tau), \quad \mathcal{L}^{-1}\left[\frac{e^{-\tau s}}{s}\right](t) = \theta(t - \tau). \quad (\text{B.3})$$

Generally, the Laplace transform is not easy to invert, and thus we would apply numerical methods to evaluate the integral (B.2). The accuracy and efficiency of different methods were tested and compared in terms of many analytic results [36, 46]. We make our choice by comparing the spectrum (with  $\alpha \rightarrow 1/\sqrt{3}$ ) obtained from direct numerical calculations with (4.7). It turns out that the Stehfest method [47] and the Piessens Gaussian Quadrature (PGQ) method [48] behave better in our cases. The Stehfest method approximates the inversion by the following sum

$$f(t) \approx \frac{\ln 2}{t} \sum_{n=1}^N c_n F\left(\frac{n \ln 2}{t}\right), \quad (\text{B.4})$$

with

$$c_n = (-1)^{n+N/2} \sum_{k=(n+1)/2}^{\min\{n, N/2\}} \frac{k^{N/2}(2k)!}{(N/2 - k)!k!(k-1)!(n-k)!(2k-n)!}, \quad (\text{B.5})$$

where  $N$  is an even number. The PGQ method is to evaluate the sum

$$f(t) \approx \frac{1}{t} \sum_{i=1}^N w_i x_i F\left(\frac{x_i}{t}\right), \quad (\text{B.6})$$

where  $x_i$  are zero points of an orthogonal polynomial  $P_i(x)$  with the recursive relation

$$\begin{aligned} P_0(x) &= 1, & P_1(x) &= x - 1, \\ P_i(x) &= \left[2(2i-1)x + \frac{2}{2i-3}\right]P_{i-1}(x) + \frac{2i-1}{2i-3}P_{i-2}(x). \end{aligned} \quad (\text{B.7})$$

And the weight is

$$w_i = (-1)^{N-1} \frac{1}{N} \left( \frac{2N-1}{x_i P_{N-1}(1/x_i)} \right)^2. \quad (\text{B.8})$$

We find that the PGQ method (figure 5) is more accurate when  $\lambda$  is close to the largest eigenvalue  $\lambda_1$ , while the Stehfest method is accurate when  $\lambda$  is not so close to  $\lambda_1$ .

## B.2 The Bell polynomials

In (4.13), we use the complete exponential Bell polynomials to express the expansion coefficients. The complete Bell polynomials have the generating function

$$B_0 = 1, \quad B_i(x_1, \dots, x_i) = \left( \frac{\partial}{\partial t} \right)^i \exp \left( \sum_{j=1}^i x_j \frac{t^j}{j!} \right) \Big|_{t=0}. \quad (\text{B.9})$$

These polynomials can also be expressed as an infinite sum of the partial exponential Bell polynomials

$$B_i(x_1, \dots, x_i) = \sum_{j=1}^i B_{i,j}(x_1, \dots, x_{i-j+1}), \quad (\text{B.10})$$

with

$$B_{i,j}(x_1, \dots, x_{i-j+1}) = \sum_{\{k\}} \frac{i!}{k_1! \cdots k_{i-j+1}!} \prod_{l=1}^{i-j+1} \left( \frac{x_l}{l!} \right)^{k_l}, \quad (\text{B.11})$$

where  $\{k\}$  means that the sum is taken over all sequences  $\{k_1 \sim k_{i-j+1}\}$  that satisfy

$$\sum_{l=1}^{i-j+1} k_l = j, \quad \sum_{l=1}^{i-j+1} l k_l = i. \quad (\text{B.12})$$

## References

- [1] M. Levin and X. G. Wen, *Detecting topological order in a ground state wave function*, [Phys. Rev. Lett. \*\*96\*\* \(2006\) 110405 \[cond-mat/0510613\]](#).
- [2] A. Kitaev and J. Preskill, *Topological entanglement entropy*, [Phys. Rev. Lett. \*\*96\*\* \(2006\) 110404 \[hep-th/0510092\]](#).
- [3] G. Vidal, J. I. Latorre, E. Rico and A. Kitaev, *Entanglement in quantum critical phenomena*, [Phys. Rev. Lett. \*\*90\*\* \(2003\) 227902 \[quant-ph/0211074\]](#).

- [4] H. Li and F. D. M. Haldane, *Entanglement spectrum as a generalization of entanglement entropy: identification of topological order in non-Abelian fractional quantum Hall effect states*, *Phys. Rev. Lett.* **101** (2008) 010504 [[arXiv:0805.0332](#)].
- [5] N. Laflorencie, *Quantum entanglement in condensed matter systems*, *Phys. Rept.* **646** (2016) 1 [[arXiv:1512.03388](#)].
- [6] L. Amico, R. Fazio, A. Osterloh and V. Vedral, *Entanglement in many-body systems*, *Rev. Mod. Phys.* **80** (2008) 517 [[quant-ph/0703044](#)].
- [7] S. Ryu and T. Takayanagi, *Holographic derivation of entanglement entropy from AdS/CFT*, *Phys. Rev. Lett.* **96** (2006) 181602 [[hep-th/0603001](#)].
- [8] S. Ryu and T. Takayanagi, *Aspects of holographic entanglement entropy*, *JHEP* **0608** (2006) 045 [[hep-th/0605073](#)].
- [9] M. Van Raamsdonk, *Building up spacetime with quantum entanglement*, *Gen. Rel. Grav.* **42** (2010) 2323 [[arXiv:1005.3035](#)].
- [10] A. Rényi, *On measures of entropy and information*, Proceedings of the 4th Berkeley Symposium on Mathematical Statistics and Probability, Vol. 1, University of California Press (1961), pp. 547–561.
- [11] P. Calabrese and A. Lefevre, *Entanglement spectrum in one-dimensional systems*, *Phys. Rev. A* **78** (2008) 032329 [[arXiv:0806.3059](#)].
- [12] L. Y. Hung, R. C. Myers, M. Smolkin and A. Yale, *Holographic calculations of Rényi entropy*, *JHEP* **1112** (2011) 047 [[arXiv:1110.1084](#)].
- [13] A. Belin, A. Maloney and S. Matsuura, *Holographic phases of Rényi entropies*, *JHEP* **1312** (2013) 050 [[arXiv:1306.2640](#)].
- [14] W. Z. Guo, *Entanglement spectrum of geometric states*, *JHEP* **02** (2021) 085 [[arXiv:2008.12430](#)].
- [15] P. Calabrese and J. Cardy, *Entanglement entropy and conformal field theory*, *J. Phys. A* **42** (2009) 504005 [[arXiv:0905.4013](#)].
- [16] P. Calabrese and J. L. Cardy, *Entanglement entropy and quantum field theory*, *J. Stat. Mech.* **0406** (2004) P06002 [[hep-th/0405152](#)].
- [17] C. Holzhey, F. Larsen and F. Wilczek, *Geometric and renormalized entropy in conformal field theory*, *Nucl. Phys. B* **424** (1994) 443-467 [[hep-th/9403108](#)].
- [18] H. Casini, M. Huerta and R. C. Myers, *Towards a derivation of holographic entanglement entropy*, *JHEP* **1105** (2011) 036 [[arXiv:1102.0440](#)].
- [19] R. Emparan, *AdS membranes wrapped on surfaces of arbitrary genus*, *Phys. Lett. B* **432** (1998) 74 [[hep-th/9804031](#)].
- [20] D. Birmingham, *Topological black holes in anti-de Sitter space*, *Class. Quant. Grav.* **16** (1999) 1197 [[hep-th/9808032](#)].
- [21] O. J. C. Dias, R. Monteiro, H. S. Reall and J. E. Santos, *A scalar field condensation instability of rotating anti-de Sitter black holes*, *JHEP* **1011** (2010) 036 [[arXiv:1007.3745](#)].
- [22] Z. Fang, S. He and D. Li, *Note on stability of new hyperbolic AdS black holes and phase transitions in Rényi entropies*, *Nucl. Phys. B* **923** (2017) 1 [[arXiv:1601.05649](#)].

- [23] C. J. Gao and S. N. Zhang, *Dilaton black holes in de Sitter or anti-de Sitter universe*, *Phys. Rev. D* **70** (2004) 124019 [[hep-th/0411104](#)].
- [24] J. Ren, *Analytic solutions of neutral hyperbolic black holes with scalar hair*, *Phys. Rev. D* **106** (2022) 086023 [[arXiv:1910.06344](#)].
- [25] C. Martínez, R. Troncoso and J. Zanelli, *Exact black hole solution with a minimally coupled scalar field*, *Phys. Rev. D* **70** (2004) 084035 [[hep-th/0406111](#)].
- [26] M. M. Caldarelli, A. Christodoulou, I. Papadimitriou and K. Skenderis, *Phases of planar AdS black holes with axionic charge*, *JHEP* **04** (2017) 001 [[arXiv:1612.07214](#)].
- [27] E. Witten, *Multitrace operators, boundary conditions, and AdS/CFT correspondence*, [hep-th/0112258](#).
- [28] X. Dong, *The gravity dual of Rényi entropy*, *Nature Commun.* **7** (2016) 12472 [[arXiv:1601.06788](#)].
- [29] M. Cvetič *et al.*, *Embedding AdS black holes in ten-dimensions and eleven-dimensions*, *Nucl. Phys. B* **558** (1999) 96 [[hep-th/9903214](#)].
- [30] S. S. Gubser and F. D. Rocha, *Peculiar properties of a charged dilatonic black hole in AdS<sub>5</sub>*, *Phys. Rev. D* **81** (2010) 046001 [[arXiv:0911.2898](#)].
- [31] C. Beck and F. Schlögl, *Thermodynamics of chaotic systems*, Cambridge University Press (1993).
- [32] Y. Nakaguchi and T. Nishioka, *A holographic proof of Rényi entropic inequalities*, *JHEP* **12** (2016) 129 [[arXiv:1606.08443](#)].
- [33] C. J. Gao and S. N. Zhang, *Higher dimensional dilaton black holes with cosmological constant*, *Phys. Lett. B* **605** (2005) 185 [[hep-th/0411105](#)].
- [34] C. J. Gao and S. N. Zhang, *Topological black holes in dilaton gravity theory*, *Phys. Lett. B* **612** (2005) 127.
- [35] A. Romero-Bermúdez, P. Sabella-Garnier and K. Schalm, *A Cardy formula for off-diagonal three-point coefficients; or, how the geometry behind the horizon gets disentangled*, *JHEP* **09** (2018) 005 [[arXiv:1804.08899](#)].
- [36] A. Cheng and P. Sidauruk, *Approximate inversion of the Laplace transform*, *The Mathematica Journal* **4** (1994) 76.
- [37] S. M. Hosseini, C. Toldo and I. Yaakov, *Supersymmetric Rényi entropy and charged hyperbolic black holes*, *JHEP* **07** (2020) 131 [[arXiv:1912.04868](#)].
- [38] T. Faulkner, G. T. Horowitz and M. M. Roberts, *Holographic quantum criticality from multi-trace deformations*, *JHEP* **04** (2011) 051 [[arXiv:1008.1581](#)].
- [39] A. Anabalón, D. Astefanesei, D. Choque and C. Martínez, *Trace anomaly and counterterms in designer gravity*, *JHEP* **03** (2016) 117 [[arXiv:1511.08759](#)].
- [40] L. Li, *On thermodynamics of AdS black Holes with scalar hair*, *Phys. Lett. B* **815** (2021) 136123 [[arXiv:2008.05597](#)].
- [41] R. M. Wald, *Black hole entropy is the Noether charge*, *Phys. Rev. D* **48** (1993) R3427 [[gr-qc/9307038](#)].
- [42] H. S. Liu and H. Lü, *Scalar charges in asymptotic AdS geometries*, *Phys. Lett. B* **730** (2014) 267 [[arXiv:1401.0010](#)].

- [43] H. Lü, C. N. Pope and Q. Wen, *Thermodynamics of AdS black holes in Einstein-Scalar gravity*, **JHEP** **03** (2015) 165 [[arXiv:1408.1514](#)].
- [44] S. A. Hartnoll, C. P. Herzog and G. T. Horowitz, *Holographic superconductors*, **JHEP** **12** (2008) 015 [[arXiv:0810.1563](#)].
- [45] R. G. Cai, L. Li and R. Q. Yang, *No inner-horizon theorem for black holes with charged scalar hairs*, **JHEP** **03** (2021) 263 [[arXiv:2009.05520](#)].
- [46] B. Davies and B. Martin, *Numerical inversion of the Laplace transform: a survey and comparison of methods*, **J. Comput. Phys.** **33** (1979) 1.
- [47] H. Stehfest, *Numerical inversion of Laplace transforms*, **Commun. ACM** **13** (1970) 47.
- [48] R. Piessens, *Gaussian quadrature formulas for the numerical integration of Bromwich's integral and the inversion of the Laplace transform*, **J. Eng. Math.** **5** (1971) 1.